Liquid Crystals
Publication details, including instructions for authors and subscription information:
http://www.informaworld.com/smpp/title~content=t713926090

Morphological phase behaviour under pressure of polycatenar mesogens with a perfluorinated moiety

Yoji Maeda[a]; Etsushi Nishikawa[a]; Hiroshi Yokoyama[a]
[a] Liquid Crystal Nanosystem Project, SORST, Japan Science and Technology Agency, Tsukuba, Ibaraki 300-2635, Japan

To cite this Article Maeda, Yoji , Nishikawa, Etsushi and Yokoyama, Hiroshi(2006) 'Morphological phase behaviour under pressure of polycatenar mesogens with a perfluorinated moiety', Liquid Crystals, 33: 8, 865 — 874
To link to this Article: DOI: 10.1080/02678290600761690
URL: http://dx.doi.org/10.1080/02678290600761690

Liquid Crystals, Vol. 33, No. 8, August 2006, 865–874

Taylor & Francis
Taylor & Francis Group

Morphological phase behaviour under pressure of polycatenar mesogens with a perfluorinated moiety

YOJI MAEDA*, ETSUSHI NISHIKAWA and HIROSHI YOKOYAMA
Liquid Crystal Nanosystem Project, SORST, Japan Science and Technology Agency, TRC 5-9-9 Tokodai, Tsukuba, Ibaraki 300-2635, Japan

(*Received 28 June 2005; in final form 9 January 2006; accepted 5 March 2006*)

Two polycatenar materials composed of a four-aromatic-ring core with a perfluorinated moiety attached in one terminal position through either butylene- or pentylene spacer groups, and three tetradecyloxy chains at the other end (abbreviated as $14PC_4F$ and $14PC_5F$), were investigated to study the effect of pressure on the phase transition behaviour. A polarizing optical microscope equipped with a high pressure optical hot stage, was used for the purpose. The T vs. P phase diagrams of $14PC_4F$ and $14PC_5F$ were constructed in the pressure region up to 100 MPa. $14PC_4F$ showed the stable crystal (Cr_1)–columnar tetragonal (Col_{tet})–smectic A (SmA)–columnar hexagonal (Col_h)–isoropic liquid (I) phase transition sequence under all pressures. $14PC_5F$ exhibited the phase sequence metastable crystal (Cr_2)–cubic (Cub)–Col_{tet}–SmA–I in a melt-cooled sample on heating under pressure. But when the melt-cooled Cr_2 sample was annealed at 52–54°C for 2–3 h, the stable crystal (Cr_1) was formed slowly, giving a stable Cr_1–Cub–Col_{tet}–SmA–I phase sequence. The temperature region of the stable cubic phase broadened with increasing pressure. Furthermore a new mesophase of $14PC_5F$ was pressure-induced between the I and SmA phases on cooling at pressures above about 16 MPa. Since the monotropic mesophase exhibited a texture very similar to that of the high temperature Col_h phase of $14PC_4F$ with planar orientation, the new phase was assigned at a high temperature columnar hexagonal phase of $14PC_5F$.

1. Introduction

Polycatenar compounds are fascinating mesogenic materials, which were first reported in 1985 by Malthete *et al.* [1]. These materials were designed to have a combined structure of rod- and disc-like mesogens, consisting of a long aromatic core and several peripheral alkyl chains [2]. A variety of mesophases, e.g. nematic, smectic, columnar and cubic, have been observed in this class of materials, resulting from the striking molecular shape and the chemical difference between hard-core parts and flexible peripheral chains [2–6]. The first polycatenar materials with a perfluorinated substituent were reported in 1991 [7, 8]. One of them was a four-ring cored tetracatenar mesogen with a perfluorooctyloxy chain, which was found to form only one liquid crystalline (LC) phase, a cubic phase [7]. Another system was a three–ring cored tricatenar material, which exhibited smectic mesomorphism [8]. Since then several polycatenar mesogens with a perfluorinated moiety have been synthesized [9]. Perfluorinated substituents incorporated into rod- and disc-like mesogens enhance microsegregation in the molecular aggregates owing to the high incompatibility with hydrocarbon parts. Accordingly, materials with perfluorinated chains tend to form LC phases with a micro-segregated structure [10–12].

We have previously reported [13–15] new tetracatenar mesogens composed of a stiff four-aromatic-ring core with a bulky, perfluorinated moiety attached to one terminal ring through an alkyl spacer of length m (m indicating the number of methylene groups in the spacer) and three tetradecyloxy chains at the other end. These are abbreviated as 14PCmF; the chemical formulae of 14PCmF with m=4 and m=5 are shown below, (scheme 1).

Polycatenar compounds usually show the lamellar (SmC)–Cub–Col phase sequence between the crystalline and isotropic liquid states [16–18]. Based on the thermal, morphological and structural characterization of compounds $14PC_4F$ and $14PC_5F$, these polycatenar materials show a rich mesomorphism strongly depending on the length of the peripheral alkyl chains [13–15]. $14PC_4F$ shows three LC mesophases between the crystalline and isotropic liquid phases, viz. a low temperature columnar tetragonal (Col_{tet}), smectic A

---

*Corresponding author. Email: maeda@nanolc.jst.go.jp

ISSN 0267-8292 print/ISSN 1366-5855 online
http://www.tandf.co.uk/journals
DOI: 10.1080/02678290600761690

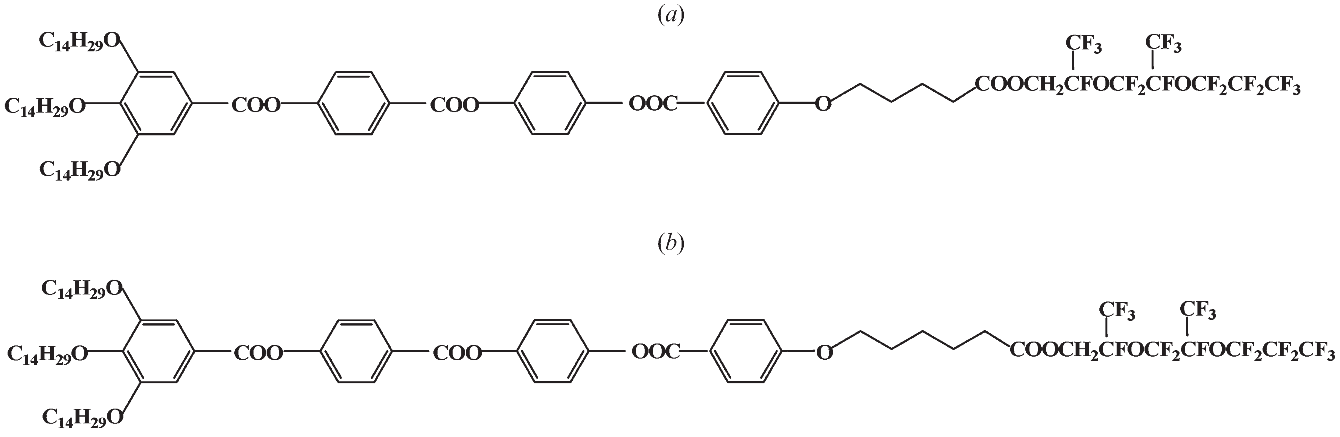

Scheme 1. Chemical formulae of (*a*) $14PC_4F$ and (*b*) $14PC_5F$.

(SmA) and a high temperature columnar hexagonal (Col_h) phase on heating. On the other hand, $14PC_5F$ shows LC polymorphism in the unique phase sequence of an optically isotropic cubic (Cub)–Col_{tet}–SmA between the stable crystal (Cr_1) and isotropic liquid (I) phases. The thermal behaviour of $14PC_5F$ on cooling, however, was complicated because of the formation of two crystalline forms and of a weakly birefringent monotropic LC phase, named here as the X phase, which was supposed to be a form of columnar phase [15], but not concluded definitely.

The phase behaviour under hydrostatic pressure of two homologous series of thermotropic cubic mesogens has been studied previously. These were 4′-*n*-hexadecyloxy-, 4′-*n*-icosyloxy-, and 4′-*n*-docosyloxy-3′-nitrobiphenyl-4-carboxylic acids—ANBC(16), ANBC(20) and ANBC(22), respectively [20–22]; and 1,2-bis-(4-*n*-alkyloxybenzoyl)hydrazines denoted BABH(*n*), where *n* indicates the number of carbon atoms in the alkoxy chain, ranging from 8 to 12 [23–25]. A high pressure differential thermal analyser (DTA), a polarizing optical microscope equipped with a high pressure hot stage and a wide angle X-ray diffractometer equipped with a high pressure sample system were used in the studies. ANBC(16) showed smectic C, cubic and smectic A phases between the crystalline and isotropic liquid phases, exhibiting the typical phase sequence Cr–SmC–Cub–SmA–I; the temperature region of the cubic phase decreased with increasing pressure up to about 50–60 MPa. The cubic phase was replaced by a new columnar phase under high pressures above about 60 MPa.

On the other hand, BABH(8) and BABH(10) showed cubic and smectic C phases at atmospheric pressure, exhibiting the Cr–Cub–SmC–I phase sequence with an inversed order of the cubic and SmC phases of ANBC(16). In BABH(8) and BABH(10), the cubic phase disappeared at very low pressures of about 30 and 10 MPa, respectively; the Cr–Cub and Cub–SmC transition lines in the *T* vs. *P* phase diagrams showed positive and negative slopes (dT/dP), respectively, and the phase diagrams exhibited triple points at very low pressures. Then BABH(8) and BABH(10) had only a SmC phase in the higher pressure region. Such intriguing phase behaviour of ANBC(16), BABH(8) and BABH(10) under pressure prompted us to study the phase behaviour of 14PC*m*F compounds under pressure, particularly focused on the effect of pressure on the phase stability of the cubic and other mesophases.

The phase behaviour of polycatenar materials with a perfluorinated substituent has rarely been studied under pressure. In this paper, we present experimental results of the morphological behaviour of two 14PC*m*F compounds with butyl ($m=4$) and pentyl ($m=5$) spacers under hydrostatic pressures up to 100 MPa using a polarizing optical microscope (POM) equipped with a high pressure optical hot stage.

2. Experimental

The synthesis of $14PC_4F$ and $14PC_5F$ samples used in this study is described elsewhere [13–15]. Morphological observation was performed using a Leiz Orthoplan polarizing optical microscope equipped with a Linkam hot stage THMS-600. X-ray diffraction patterns of the samples were measured using a wide angle X-ray diffractometer (RAXIS-IV, Rigaku Co., Ltd). A Ni-filtered Cu K_α X-ray beam was used to irradiate the sample, and the diffraction patterns were obtained using an imaging plate detector.

Morphological observation under pressure was performed using the Leiz microscope equipped with a high pressure optical hot stage, as described elsewhere [26, 27]. The high pressure optical hot stage equipped with two sapphire windows was used in a temperature region between room temperature and 160°C under hydrostatic pressures up to 100 MPa. Dimethylsilicone oil with a low viscosity (10 cSt) was used as the pressurizing medium. A thin film of the sample was prepared between miniature slide-glasses ($5 \times 7\,\mathrm{mm}^2$) which were set in a steel holder; the steel holder was inserted into the high pressure optical cell. The sample sandwiched between the slide-glasses was pressurized hydrostatically; direct contact of the sample with silicone oil was avoided except for the edges. The texture observation was performed at an average heating and cooling rates of $1^{\circ}\mathrm{C\,min}^{-1}$ under various pressures.

3. Results and discussion

3.1. *Phase behaviour and texture of the monotropic Col_h phase of $14PC_5F$ under pressure*

The thermodynamic quantities associated with the phase transitions of $14PC_4F$ and $14PC_5F$ have been reported elsewhere [13–15, 19]. In brief, additional facts for $14PC_4F$ and $14PC_5F$ are that both the metastable and stable crystals were usually formed with the supercooled or glassy state of the Col_{tet} phase during cooling. DSC curves on subsequent heating show the glass transition of the quenched Col_{tet} phase and a large exothermic peak of crystallization at about 46 and 51–56°C, respectively. The transition schemes for both compounds are summarized in scheme 2.

Since the (unknown) X phase appeared only on cooling, this phase is regarded as a thermodynamically unstable phase because there are stable Cr_1 and cubic phases in the same temperature region. The X phase may be composed of a major portion of the supercooled Col_{tet} phase and a minor portion of crystals, probably involving a nucleation process. When the melt-cooled Cr_2 sample was annealed for a couple of hours at temperatures around the Cr_2–Cub transition, Cr_1 stable crystals grew slowly by a melt-crystallization mechanism. The temperature range of the stable cubic phase of the annealed $14PC_5F$ sample is only about 2°C at atmospheric pressure.

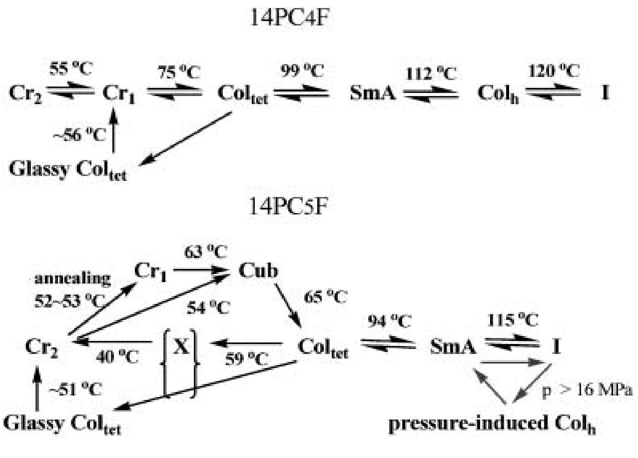

Scheme 2. Phase transition sequences of $14PC_4F$ and $14C_5F$.

Since the DSC peaks of the Cub–Col_{tet}, Col_{tet}–SmA and SmA–Col_h transitions of $14PC_4F$ and $14PC_5F$ were barely detected by high pressure DTA, texture observation by POM with a high pressure hot stage was adopted in this study. Although the contrast in image of the textures of these mesophases under hydrostatic pressure was lower, compared with the usual POM images at atmospheric pressure, texture observation and optical measurements were still effective for the qualitative identification of the mesophases under pressure.

Figure 1 shows the textures of $14PC_4F$ on cooling from the isotropic liquid at 22 and 33 MPa. A "pleated fan" texture for the Col_h phase was observed from the isotropic liquid at 22 MPa, figure 1 (*a*). At 33 MPa, either pleated fan or focal-conic fan textures characteristic of the Col_h phase were observed at 115 and110°C, figures 1 (*b*) and 1 (*c*), respectively; these textures were held at temperatures down to about 90°C. On further cooling another fine texture was seen at 70°C, figure 1 (*d*), indicating the formation of the low temperature Col_{tet} phase [15]. These textures were commonly observed on cooling at high pressures.

On cooling a sample of $14PC_5F$ at atmospheric pressure, the black field of view for the isotropic liquid was retained in the SmA phase due to homeotropic alignments [13–15]. The characteristic texture of the Col_{tet} phase appeared clearly at low temperatures below the SmA–Col_{tet} transition at 94°C. When hydrostatic pressure above about 16 MPa was applied to the $14PC_5F$ sample, a new texture appeared at first between the isotropic liquid and the SmA phase on cooling. Figure 2 shows the POM textures of $14PC_5F$ on cooling from the isotropic liquid at 23 MPa. A dark-yellow field of view was observed for the isotropic liquid at 123°C, figure 2 (*a*). Then a new texture with many small-rod aggregates was observed at 115°C, figure 2 (*b*), which was very similar to the texture of the planar-oriented columnar hexagonal Col_h phase of $14PC_4F$ sandwiched between polyimide-coated glass plates [15]. The small rod-like texture of $14PC_5F$ is refered to as a pressure-induced Col_h phase. The columnar texture disappeared at about 112°C, and the field of view became dark due to the homeotropic alignment of the SmA phase at 110°C, figure 2 (*c*). The homeotropic SmA phase was held at

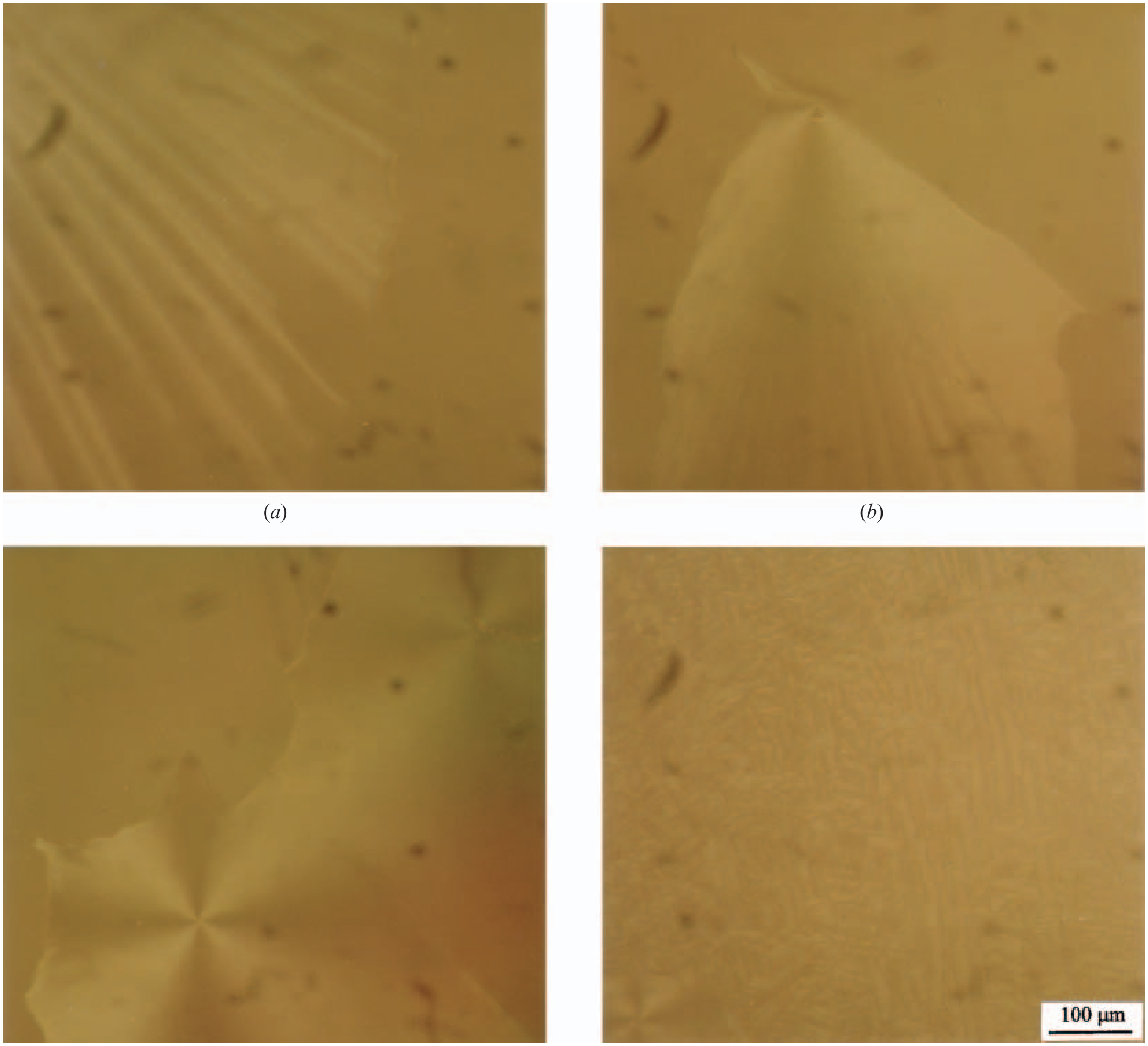

Figure 1. POM micrographs of textures of $14PC_4F$ observed on cooling at 22 and 33 MPa: (*a*) Col_h phase at 125°C and 22 MPa, (*b*) Col_h phase at 115°C and 33 MPa, (*c*) Col_h phase at 110°C and 33 MPa, (*d*) Col_{tet} phase at 70°C and 33 MPa.

temperatures down to about 90°C. On further cooling, a fine texture with many parallel striations of the columnar tetragonal phase was observed at 80°C, figure 2 (*d*). The texture of the columnar tetragonal phase then changed to that of a low temperature LC phase; i.e. the unknown X phase, at about 68°C, figure 2 (*e*). The texture of the X phase was seen at lower temperatures such as 43°C, figure 2 (*f*). The changes in texture of $14PC_5F$ mentioned above were confirmed by simultaneous observation of transmitted light intensity for the determination of the transition points on heating and cooling processes.

Figure 3 shows examples of the *I* vs. *T* curves of (*a*) melt-cooled $14PC_4F$ and (*b*) annealed $14PC_5F$ on heating and subsequent cooling runs at 50 MPa. The Cr_1–Col_{tet} and Col_h–I transitions of $14PC_4F$ were observed reversibly, while the Col_{tet}–SmA and SmA–Col_h transitions were seen only on cooling. In $14PC_5F$ the Cr_1 stable crystal, formed by annealing melt-cooled Cr_2 crystals at 54°C for 2.5 h at atmospheric pressure,

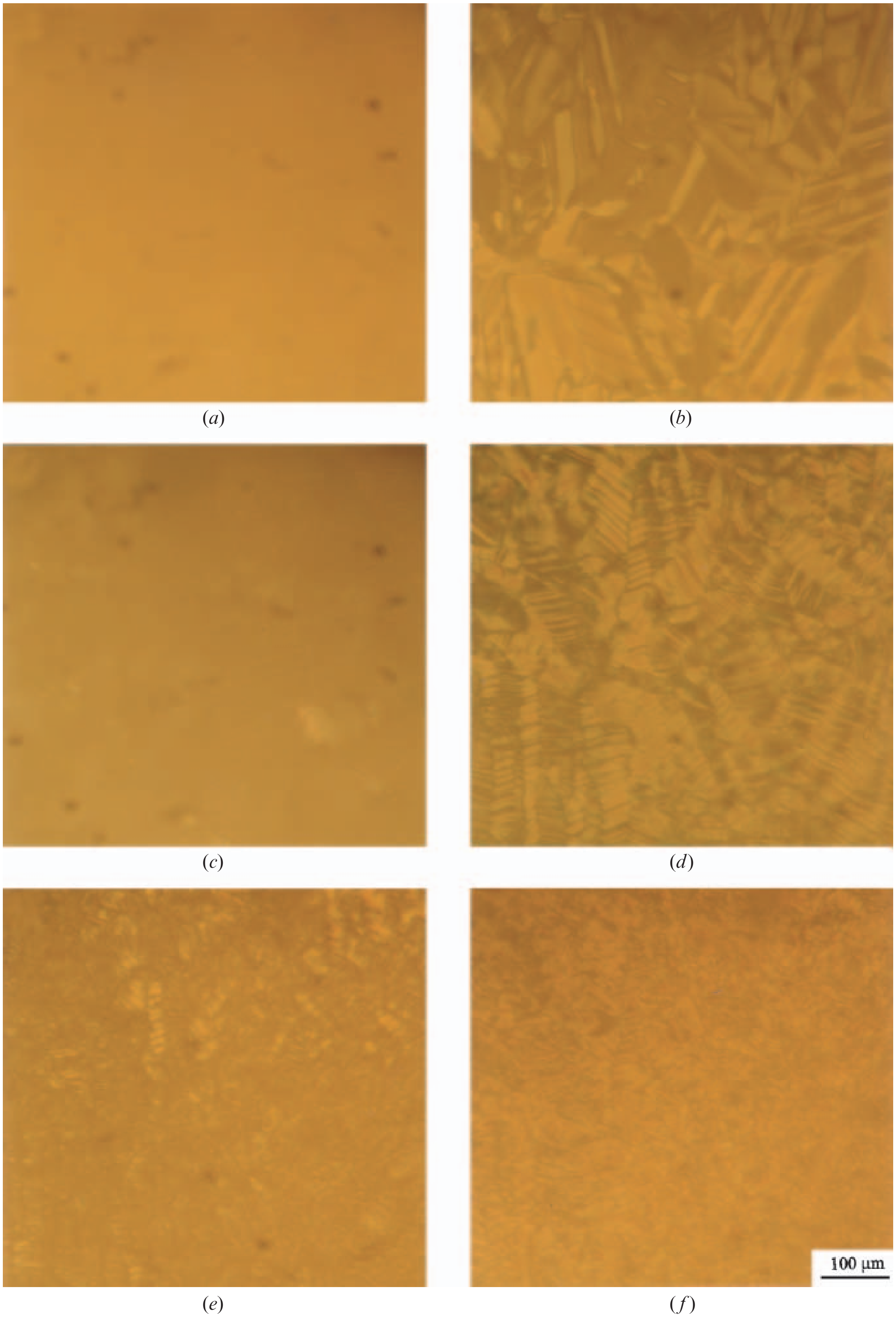

Figure 2. POM micrographs of textures of $14PC_5F$ on cooling from the isotropic liquid at 23 MPa: (*a*) isotropic liquid at 123°C, (*b*) monotropic Col_h phase at 115°C, (*c*) homeotropic SmA phase at 110°C, (*d*) Col_{tet} phase at 80°C, (*e*) Col_{tet}–X transition at 68°C, (*f*) X phase at 43°C.

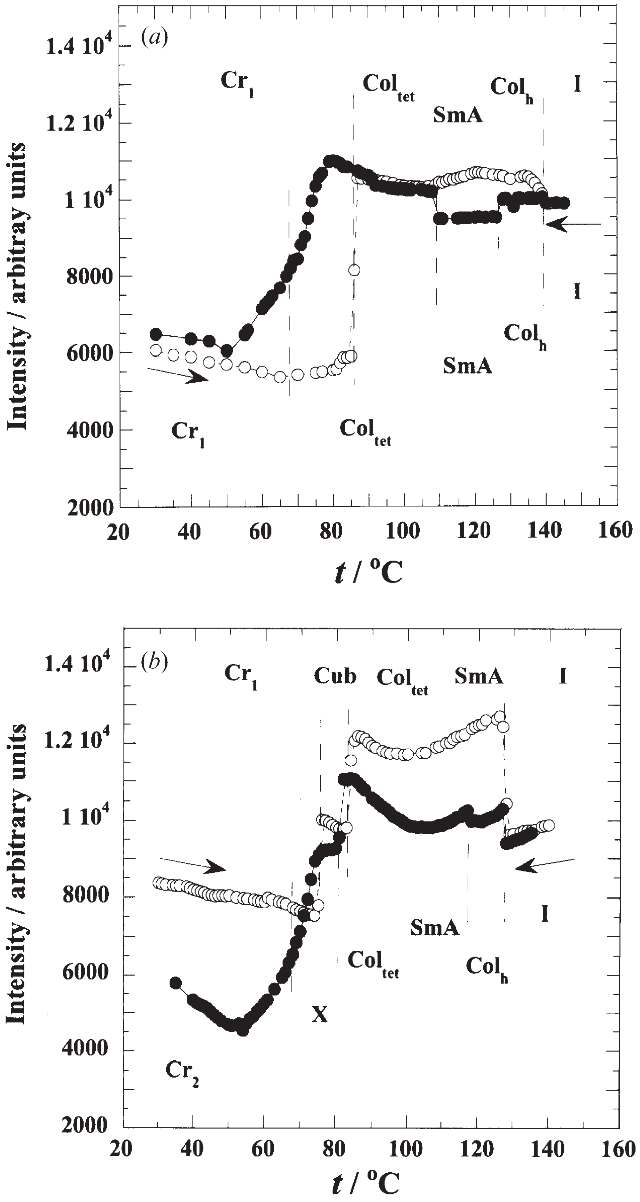

Figure 3. *I* vs. *T* curves of (*a*) 14PC$_4$F and (*b*) annealed 14PC5F on heating and subsequent cooling at 50 MPa. 14PC$_5$F had been crystallized into the Cr$_1$ phase by annealing at 54°C for 2.5 h at atmospheric pressure.

was used as the starting material. One can see the Cr$_1$–Cub, Cub–Col$_{tet}$ and SmA–I transitions on heating under pressures, but not the Col$_{tet}$–SmA transition. We note here that the cubic phase can be recognized clearly between the Cr$_1$ and Col$_{tet}$ phases on heating under pressure and that the X phase also appears on subsequent cooling. Furthermore, the presence of a pressure-induced, monotropic Col$_h$ phase was recognized in the *I* vs. *T* curve of 14PC$_5$F at 50 MPa.

3.2. *T vs. P phase diagrams of 14PC$_4$F and 14PC$_5$F*

Figures 4 and 5 show the *T* vs. *P* phase diagrams of 14PC$_4$F and annealed 14PC$_5$F on heating in the pressure range up to 100 MPa. The transition curves between the stable phases of 14PC$_4$F, except for the Col$_{tet}$–SmA transition, can be expressed as first order

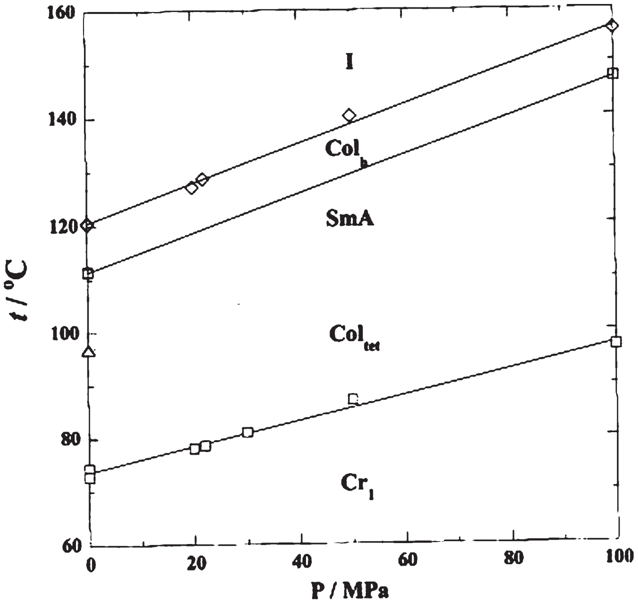

Figure 4. *T* vs. *P* phase diagram of 14PC$_4$F.

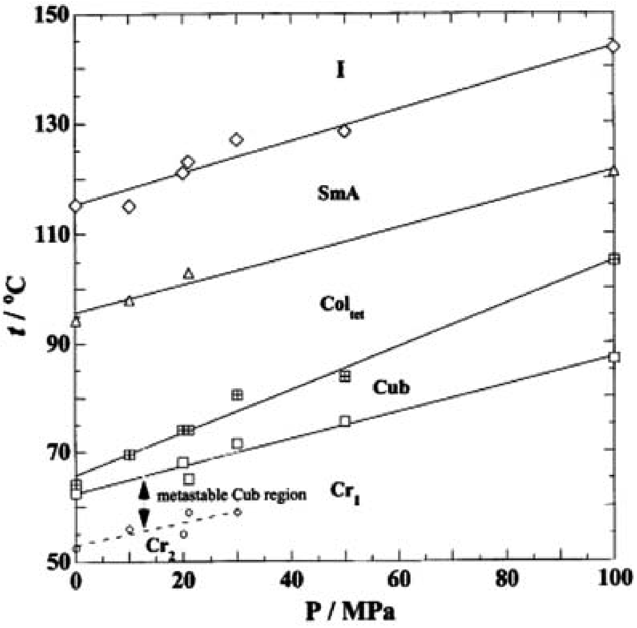

Figure 5. *T* vs. *P* phase diagram of a 14PC$_5$F sample which had been annealed at 54°C for 2.5 h at atmospheric pressure.

polynomials in terms of pressure as follows:

14PC$_4$F (T/°C: peak temperature)
Transition
$\mathrm{Cr_1{\to}Col_{tet}}$ $T/{}^\circ\mathrm{C}=73.6+0.240\,(P/\mathrm{MPa})$
$\mathrm{Col_{tet}{\to}SmA}$ ……………………………
$\mathrm{SmA{\to}Col_h}$ $T/{}^\circ\mathrm{C}=111.4+0.356\,(P/\mathrm{MPa})$
$\mathrm{Col_h{\to}I}$ $T/{}^\circ\mathrm{C}=120.5+0.361\,(P/\mathrm{MPa})$.

The $\mathrm{Cr_1}$–$\mathrm{Col_{tet}}$–SmA–$\mathrm{Col_h}$–I phase sequence at atmospheric pressure was maintained under hydrostatic pressures up to 100 MPa. All the transition curves of 14PC$_4$F and 14PC$_5$F have positive slopes ($\mathrm{d}T/\mathrm{d}P$) in the whole pressure region studied. The 14PC$_5$F sample annealed at 54°C for 2.5 h under atmospheric pressure was used as a starting material. The transition curves can be expressed as first order polynomials in terms of pressure as follows.

14PC$_5$F (T/°C: peak temperature)
Transition
$\mathrm{Cr_1{\to}Cub}$ $T/{}^\circ\mathrm{C}=62.4+0.250\,(P/\mathrm{MPa})$
$\mathrm{Cub{\to}Col_{tet}}$ $T/{}^\circ\mathrm{C}=65.6+0.395\,(P/\mathrm{MPa})$
$\mathrm{Col_{tet}{\to}SmA}$ $T/{}^\circ\mathrm{C}=95.6+0.257\,(P/\mathrm{MPa})$
$\mathrm{SmA{\to}I}$ $T/{}^\circ\mathrm{C}=115.3+0.286\,(P/\mathrm{MPa})$.

The T vs. P phase diagram of 14PC$_5$F during heating exhibits a stable cubic phase between the $\mathrm{Cr_1}$ and $\mathrm{Col_{tet}}$ phases at all pressures. It is interesting to see that the temperature range of the cubic phase broadens with increasing pressure. The transition line of the metastable $\mathrm{Cr_2}$ phase is shown as a dotted line for reference. Figure 6 shows the T vs. P phase diagram of 14PC$_5$F measured during cooling. The I–SmA–$\mathrm{Col_{tet}}$–X(–$\mathrm{Cr_2}$) phase sequence was observed at pressures below about 16 MPa. Applying pressure above 16 MPa, however, induced the monotropic $\mathrm{Col_h}$ phase between the isotropic liquid and the SmA phase, and the I–$\mathrm{Col_h}$–SmA–$\mathrm{Col_{tet}}$–X(–$\mathrm{Cr_2}$) phase sequence was observed at higher pressures. Subsequent heating, however, showed the $\mathrm{Cr_2}$–Cub–$\mathrm{Col_{tet}}$–SmA–I phase sequence, without the $\mathrm{Col_h}$ phase, at the same pressure. It is concluded at this stage that the monotropic, high temperature columnar hexagonal $\mathrm{Col_h}$ phase of 14PC$_5$F, very similar to the texture of the planar oriented $\mathrm{Col_h}$ phase of 14PC$_4$F, is induced between the isotropic liquid and the SmA phase on cooling under pressures above about 16 MPa.

3.3. *Observation of the cubic phase of 14PC$_5$F under pressure*

Figure 7 shows the X-ray diffraction pattern of a 14PC$_5$F sample at 62°C under atmospheric pressure. The X-ray pattern shows several strong spots on one or two weak Debye rings at low angles and a diffuse halo at wide angles, indicating the typical diffraction pattern of the cubic structure [28]. Thus the existence of a stable cubic phase on heating at atmospheric pressure was confirmed structurally. We observed directly the texture

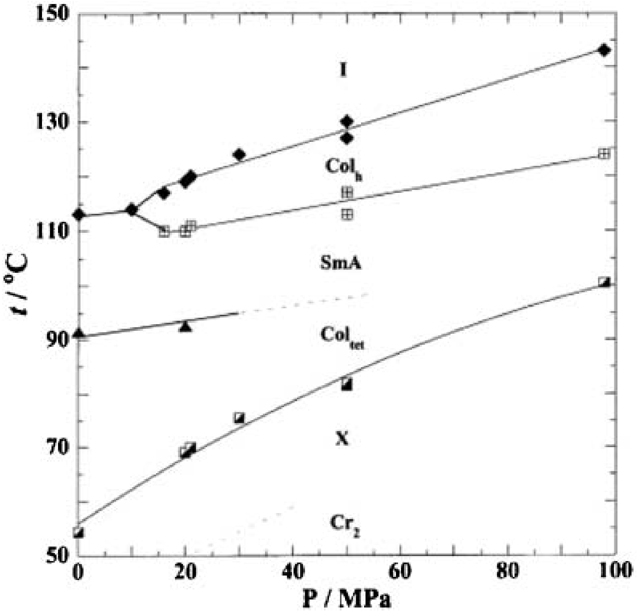

Figure 6. T vs. P phase diagram of 14PC$_5$F obtained during cooling.

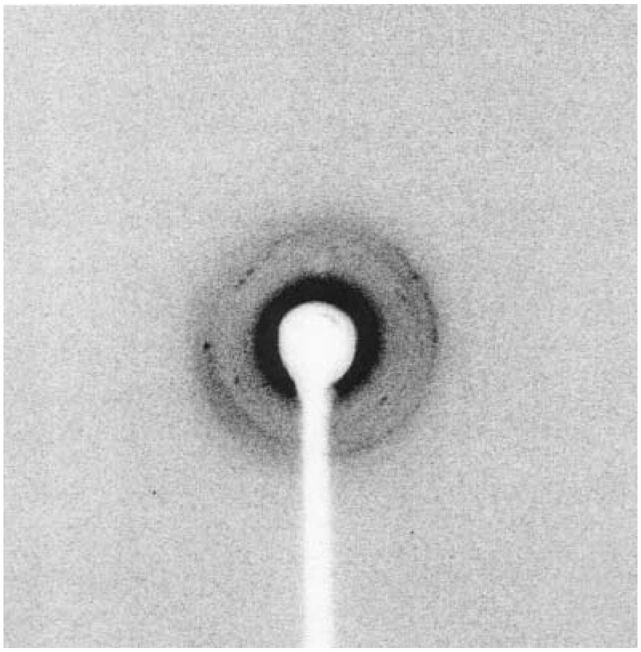

Figure 7. X-ray diffraction pattern of the cubic phase of 14PC$_5$F at 62°C at atmospheric pressure. The strong spots on one or two circular rings seem to be reflections of the cubic structure with the *Im*3*m* space group.

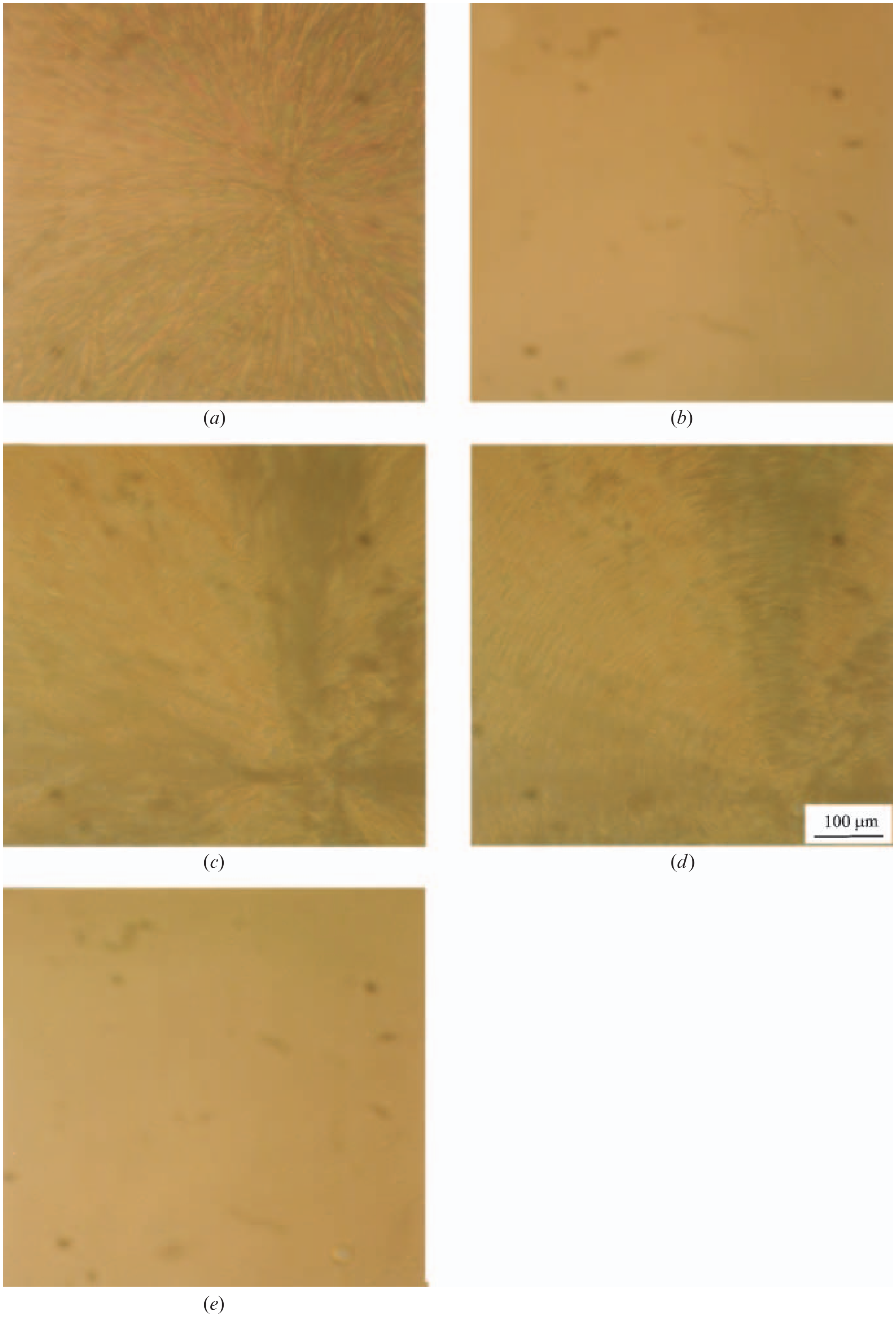

(a) (b) (c) (d) (e)

Figure 8. POM micrographs of the texture of an annealed sample of 14PC$_5$F on heating at 30 MPa: (*a*) Cr$_1$ at 60°C, (*b*) cubic phase at 72°C, (*c*) Col$_{tet}$ phase at 80°C, (*d*) SmA phase at 116°C, (*e*) isotropic liquid at 124°C.

of the cubic phase of 14PC$_5$F under pressure. Figure 8 shows POM micrographs of the texture of an annealed 14PC$_5$F sample on heating at 30 MPa. The Cr$_1$ crystal, prepared by annealing the melt-cooled sample at 54°C for 2.5 h under atmospheric pressure, showed a large spherulite at temperatures between room and about 70°C, as shown in figure 8 (*a*) for the crystal spherulite at 60°C. On heating the crystal, the dark-yellow field of view for the cubic phase appeared at temperatures between 70 and 80°C; the cubic phase at 72°C is shown in figure 8 (*b*). A typical texture for the Col$_{tet}$ phase then appeared at 80°C, figure 8 (*c*); afterwards the texture did not change significantly, figure 8 (*d*), until isotropization occurred at 124°C, figure 8 (*e*). Based on the microscopic observations, it is concluded that a stable cubic phase exists between the crystal and columnar tetragonal phases and that its temperature range broadens with increasing pressure.

The Cr$_1$–Cub–Col$_{tet}$–SmA–I phase sequence of 14PC$_5$F is held during heating under all pressures. On the other hand, a monotropic 14PC$_5$F mesophase, very similar to the high temperature columnar hexagonal Col$_h$ phase of 14PC$_4$F with planar orientation, was found between the isotropic liquid and the SmA phase on cooling under pressures above about 16 MPa; the Col$_h$ phase was not observed on subsequent heating at the same pressure. At present we have no reasonable explanation for the appearance of a monotropic Col$_h$ phase under pressures above about 16 MPa. We suggest the possibility that pressure would promote 14PC$_5$F taking the same phase transition sequence as the Col$_{tet}$–SmA–Col$_h$ sequence of 14PC$_4$F. We hope for a solution of this problem in the future.

Recently, we reported the phase diagram showing a stable thermotropic cubic phase of 4-(ethylpentoxy) anilinebenzylidene-4′-carboxylic acid (EPABC) under pressures up to about 250 MPa [29]. This mesogenic system showed the stable cubic phase and the Cr–Cub–I phase sequence under all pressures. The existence of stable cubic phases under pressure is reported for several lyotropic liquid crystals, such as saturated didodecyl and ditetradecyl phosphatidylethanolamines (DDPE and DTPE), in which an increase of pressure stabilized inverse bicontinuous cubic phases with *Im*3*m* and *Pn*3*m* cubic structures in DTPE [30]. Other examples of the phase behaviour of fatty acid/phosphatidylcholine (FA/PC) in excess water were reported by Winter *et al.* [31]. The *P*–*T* phase diagrams of 2:1 FA/PC mixtures in excess water, viz. lauric acid (LA)/1,2-dilauroyl-*sn*-glycero-3- phosphatidylcholine (DLPC) and myristic acid (MA)/1,2-dimyristoyl-*sn*-glycero-3-phosphatidylcholine (DMPC) systems showed positive slopes (dT/dP) of the L_α–Q^P and Q^P–Q^D for the former, and of the L_β–H_{ii}/Q^P phase transition for the latter system. So the stable cubic phase under pressure seems to be widespread, and the thermotropic cubic mesogens of ANBC(16), BABH(8) and BABH(10) under pressure seems to be exceptional, wherein the cubic phases are destabilized by applying pressure and finally disappear under elevated pressures [20–25]. The difference in stability of the cubic phase with pressure may be caused by the difference in cubic structures between these compounds. 14PC$_5$F and other polycatenar compounds take the *Im*3*m* space group with a discontinuous micelle-type body-centered cubic structure [4, 9]. On the other hand, the thermotropic cubic mesogens of ANBC(*n*) and BABH(*n*) compounds have the *Ia*3*d* space group with a bicontinuous interwoven network structure. The discontinuous body-centered cubic structure with the *Im*3*m* symmetry would be generally stable under pressure, similar to the lyotropic cubic liquid crystals mentioned above.

4. Conclusion

The transition behaviour of polycatenar compounds 14PC$_4$F and 14PC$_5$F, which have three peripheral tetradecyloxy chains at one end of the molecule and a bulky perfluorinated moiety through a spacer group –O(CH$_2$)$_m$COO– (m=4 and 5) at the other end, were investigated under pressures up to 100 MPa using a polarizing optical microscope equipped with a high pressure optical hot stage. The temperature vs. pressure phase diagrams of 14PC$_4$F and 14PC$_5$F were constructed. 14PC$_4$F showed reversibly the Cr$_1$–Col$_{tet}$–SmA–Col$_h$–I phase sequence under all pressures. 14PC$_5$F showed the stable phase sequence Cr$_1$–Cub–Col$_{tet}$–SmA–I on heating under all pressures. However, a monotropic columnar hexagonal phase appeared between the isotropic liquid and SmA phase under pressures above about 16 MPa, showing the I–Col$_h$–SmA–Col$_{tet}$–X(–Cr$_2$) phase sequence, the same as for 14PC$_4$F except for the appearance of the X phase and different crystallization kinetics. It is concluded that 14PC$_5$F exhibits a stable cubic phase on heating under all pressures.

References

[1] J. Malthete, A.M. Levelut, H.T. Nguyen. *J. Phys. (Paris) Lett.*, **46**, L875 (1985).
[2] J. Malthete, H.T. Nguyen, C. Destrade. *Liq. Cryst.*, **13**, 171 (1993).
[3] A.M. Levelut, J. Malthete, C. Destrade, H.T. Nguyen. *Liq. Cryst.*, **2**, 877 (1987).
[4] K.E. Rowe, D.W. Bruce. *J. mater. Chem.*, **8**, 331 (1998).
[5] M.-A. Guillevic, T. Gelbrich, M.B. Hursthouse, D.W. Bruce. *Mol. Cryst. liq. Cryst.*, **362**, 147 (2001).

[6] D. Fazio, C. Mongin, B. Donnio, Y. Galerne, D. Guillon, D.W. Bruce. *J. mater. Chem.*, **11**, 2852 (2001).

[7] H.T. Nguyen, G. Sigaud, M.F. Achard, F. Hardouin, R.J. Twieg, K. Betterton. *Liq. Cryst.*, **10**, 389 (1991).

[8] T. Doi, Y. Sakurai, A. Tamatani, S. Takenaka, S. Kusabayashi, Y. Nishihata, Y. Teraushi. *J. mater. Chem.*, **1**, 169 (1991).

[9] H.T. Nguyen, C. Destrade, J. Malthete. In *Handbook of Liquid Crystals*, Vol. 2B, 865, D. Demus, J.W. Goodby, G.W. Gray, H.W. Spiess, V. Vill (Eds), Wily-VCH, Weinheim (1998).

[10] T.A. Lobko, B.I. Ostrovskii, A.I. Pavluchenko, S.N. Sulianov. *Liq. Cryst.*, **15**, 361 (1993).

[11] S. Diele, D. Lose, H. Kruth, G. Pelzl, F. Guittard, A. Cambon. *Liq. Cryst.*, **21**, 603 (1996).

[12] D. Lose, S. Diele, G. Pelzl, E. Dietzmann, W. Weissflog. *Liq. Cryst.*, **24**, 707 (1998).

[13] E. Nishikawa, J. Yamamoto, H. Yokoyama. *Chem. Commun.*, 420 (2003).

[14] E. Nishikawa, J. Yamamoto, H. Yokoyama. *J. mater. Chem.*, **13**, 1887 (2003).

[15] E. Nishikawa, J. Yamamoto, H. Yokoyama. *Liq. Cryst.*, **32**, 585 (2005).

[16] K. Hiltrop. In *Liquid Crystals*, p. 143, H. Baumgärtel, E.U. Franck, W. Grunbein, H. Stegemeyer (Eds), Steinkopff, Darmstadt (1994).

[17] C.M. Paleos, D. Kardassi, D. Tsiourvas, A. Skoulios. *Liq. Cryst.*, **25**, 267 (1998).

[18] K. Borisch, S. Diele, P. Göring, H. Müller, C. Tschierske. *Liq. Cryst.*, **22**, 427 (1997).

[19] K. Saito, D. Kanki, S. Ikeuchi, E. Nishikawa, J. Yamamoto, H. Yokoyama, In proceeding of the *20th International Liquid Crystal Conference*, 4–9 July, 2004, Ljubljana, Slovenia, MAC-P007.

[20] Y. Maeda, G.-P. Cheng, S. Kutsumizu, S. Yano. *Liq. Cryst.*, **28**, 1785 (2001).

[21] Y. Maeda, S.K. Prasad, S. Kutsumizu, S. Yano. *Liq. Cryst.*, **30**, 7 (2003).

[22] Y. Maeda, K. Morita, S. Kutsumizu. *Liq. Cryst.*, **30**, 157 (2003).

[23] Y. Maeda, K. Saito, M. Sorai. *Liq. Cryst.*, **30**, 1139 (2003).

[24] Y. Maeda, T. Ito, S. Kutsumizu. *Liq. Cryst.*, **31**, 623 (2004).

[25] Y. Maeda, T. Ito, S. Kutsumizu. *Liq. Cryst.*, **31**, 807 (2004).

[26] Y. Maeda, M. Koizumi. *Rev. sci. Instrum.*, **67**, 2030 (1996).

[27] Y. Maeda, M. Koizumi. *Rev. high pressure Sci. Technol.*, **7**, 1532 (1998).

[28] S. Fischer, H. Fischer, S. Diele, G. Pelzl, K. Jankowski, R.R. Schmidt, V. Vill. *Liq. Cryst.*, **17**, 855 (1994).

[29] Y. Maeda, T. Niori, J. Yamamoto, H. Yokoyama. *Thermochim. Acta.*, **428**, 57 (2005).

[30] P.M. Duesing, J.M. Seddon, R.H. Templer, D.A. Mannock. *Langmuir*, **13**, 2655 (1997).

[31] R. Winter, J. Erbes, R.H. Templer, J.M. Seddon, A. Syrykh, N.A. Warrender, G. Rapp. *Phys. Chem. chem. Phys.*, **1**, 887 (1999).